Cement & Concrete Composites 34 (2012) 650–662

Contents lists available at SciVerse ScienceDirect

Cement & Concrete Composites

journal homepage: www.elsevier.com/locate/cemconcomp

Use of nano-silica to increase early strength and reduce setting time of concretes with high volumes of slag

Min-Hong Zhang [a],*, Jahidul Islam [a], Sulapha Peethamparan [b]

[a] Department of Civil and Environmental Engineering, National University of Singapore, 1 Engineering Drive 2, 117576 Singapore, Singapore
[b] Department of Civil and Environmental Engineering, Clarkson University, 8 Clarkson Avenue, Potsdam, NY 13699-710, USA

ARTICLE INFO

Article history:
Received 15 July 2011
Accepted 7 February 2012
Available online 23 February 2012

Keywords:
Compressive strength
Nano-silica
Pore-size distribution
Rate of cement hydration
Setting time
Silica fume
Slag

ABSTRACT

The effects of nano-silica (NS) on setting time and early strengths of high volume slag mortar and concrete have been experimentally studied. Effects of NS dosages, size and dispersion methods on strength development of high volume slag mortars were also investigated. A constant water-to-cementitious materials ratio (w/cm) 0.45 was used for all mixtures. The results indicate that the incorporation of a small amount of NS reduced setting times, and increased 3- and 7-day compressive strengths of high-volume slag concrete, significantly, in comparison to the reference slag concrete with no silica inclusion. Compressive strength of the slag mortars were increased with the increase in NS dosages from 0.5% to 2.0% by mass of cementitious materials at various ages up to 91 days. The strengths of the slag mortars were generally increased with the decrease in the particles size of silica inclusions at early age. Ultra-sonication of nano-silica with water is probably a better method for proper dispersion of nano-silica than mechanical mixing method.

1. Introduction

Ground granulated blast-furnace slag (GGBFS) has been used in concrete for many years either as a supplementary cementing material added in concrete batching plants or as a component added in production of blended cements. Concretes with high percentages (>50%) of GGBFS have been used for applications in marine environments and situations where ground water has high sulfate contents. Concretes with high percentages of slag can develop good strengths over time, exceeding those of similar concretes without slag. However, such concretes often have lower early strength and longer setting time than Portland cement concrete without slag.

In recent years several researches show that early-age and 28-day strengths of cement pastes [1], mortars [2,3], and concrete [4] are increased by using a small amount of nano-silica (NS). Higher strengths of mixtures with NS in comparison to those with silica fume are also reported for mortars [2,3] and concrete [4]. The higher strengths are attributed to accelerated cement hydration [1,4], reduced pores [2], and improved interface bonding between hardened cement paste and aggregate [1]. Nano-silica has also been used to increase early strength of concrete with fly ash [5,6]. However, no information is available on whether NS can be used to decrease setting time and increase early strength of concrete with high volumes of GGBFS.

This paper presents an experimental study on the use of NS to improve setting time and early strengths of slag mortar and concrete. Two types of nano-silica with specific surfaces of 200.1 and 321.6 m^2/g were included in the study in comparison to silica fume with a specific surface of 21.3 m^2/g. Effect of NS dosages and dispersion methods were also investigated. In addition to the compressive strength and setting time, rate of heat development of cement pastes in the first 30 h, pore structure of the cement pastes, and microstructure of the concrete at 28 days were also studied. Effect of NS on concrete resistance to chloride-ion penetration at 28 days was determined according to ASTM C 1202 [7] test.

2. Experimental details

In this study specimens were prepared to determine effect of dosage, particle size, and dispersion method of NS on compressive strength of mortars (from 1 to 91 days) with about 50% GGBFS. A superplasticizer was used to achieve target flow from 104% to 111% of the mortars. Cement pastes with the same w/cm and mix proportion as the mortars (except for the sand) were prepared to determine the rate of heat development and cement hydration in the first 30 h, and pore structure at 28 days. Selected concrete mixtures were prepared to determine the effect of NS on setting time, compressive strength development from 3 to 91 days and resistance to chloride-ion penetration at 28 days in comparison

---

* Corresponding author. Tel.: +65 6516 2273; fax: +65 6779 1635.
E-mail addresses: ceezmh@nus.edu.sg (M.-H. Zhang), jahidul.isl@gmail.com (J. Islam), speetham@clarkson.edu (S. Peethamparan).

0958-9465/$ - see front matter © 2012 Elsevier Ltd. All rights reserved.
doi:10.1016/j.cemconcomp.2012.02.005

to the reference slag concrete without the inclusion and the concrete with silica fume.

2.1. Materials

Normal Portland Cement and ground granulated blast-furnace slag were used for various mortars and concretes. Two types of NS with different specific surface areas and average particle sizes were used in this study in comparison to silica fume. Characteristics of these materials are given in Table 1. Type 1 and Type 2 NS had specific surface areas of 200.1 and 321.6 m^2/g, respectively, in comparison to 21.3 m^2/g of the silica fume. A polycarboxylate based superplastisizer was used in mortar, paste, and concrete mixtures for workability purposes. Natural sand with a fineness modulus of 2.97 was used for mortar and concrete mixtures. Crushed granite coarse aggregate with a maximum aggregate size of 20 mm was used for concrete mixtures. Both the coarse and fine aggregates met the requirements of ASTM C 33 [8]. Tap water was used for mortar and concrete mixing, whereas deionized water was used for cement pastes.

2.2. Mortar and concrete mixtures

2.2.1. Mix proportions

Eight mortar mixtures were included in the study (Tables 2–4). All the mortars had a water-to-cementitious materials ratio (w/cm) of 0.45 and a sand-to-cementitious materials ratio of 2.75. Dosages of the Type 1 NS varied from 0 to 0.5%, 1.0% and 2.0% by mass of the cementitious materials (Table 2). Mortars with 1% Type 1 or Type 2 NS were compared with that with the same amount of silica fume to evaluate the effect of specific surface area and particle size of silica (Table 3). As the NS particles were extremely fine, influences of mixing and dispersing methods on properties of the mortars were also evaluated (Table 4).

In addition to the mortars, effect of NS on concrete properties was studied in comparison to that of silica fume. Mix proportions of the concretes are given in Table 5.

2.2.2. Specimen preparation, curing, and testing

2.2.2.1. Mortars. Mortars were mixed in a Hobart mixer at an ambient temperature of about 30 °C. For mortar mixtures with mechanical mixing, solid materials were dry mixed first. Water was added and mixed for 1 min followed by addition of superplasticizer and mixed for 1 more min at low speed and 30 s at high speed. The superplasticizer was used to achieve the target flow from 104% to 111%. The flow value was determined according to ASTM C 1437 [9].

For ultrasonic mixing, NS and water were mixed first using ultrasonic mixer with 90 Watts power input for 5 min. The sonicated mixture was then mixed in a Hobart mixer with sand, cement and slag for 1 min. After that, superplasticizer was added and mixed for 1 min at low speed and 30 s at high speed.

For each mortar mixture, fifteen 50 × 50 × 50-mm specimens were cast for compressive strength test. The molded specimens were covered with wet burlap for the first 24 h to prevent moisture loss. After demold, the specimens were cured in a fog room at a temperature of about 28–30 °C until the time of testing. Compressive strengths of the mortars were determined at 1, 3, 7, 28, and 91 days according to ASTM C 109/C 109M [10].

2.2.2.2. Concretes. Concretes were mixed using a pan mixer at an ambient temperature of about 30 °C. Before concrete mixing, NS or silica fume were mixed with water using the ultrasonic mixer for adequate dispersion of the particles. The sonicated mixture was then mixed with aggregate, slag and cement in the pan mixer for 1 min. The superplasticizer was added and mixed for another 1–2 min to achieve a target slump of about 100 mm.

Twelve 100-mm cubes and one 100 × 200-mm cylinders were cast for each concrete mixture for determining compressive strength and chloride-ion penetrability, respectively. Mortar sieved from the concrete was used to cast a 150-mm cube to determine setting time of concrete. Compressive strengths of concretes were determined at 3, 7, 28, and 91 days according to BS EN 12390-3 [11], setting time of concretes were determined according to ASTM C 403/C 403M [12], and resistances to chloride-ion penetration were determined at 28 days according to ASTM C 1202 [7]. Curing of the concretes was the same as that of the mortar specimens.

2.3. Cement paste mixtures

2.3.1. Mix proportions and mixing

Mix proportions of cement pastes were similar to those of the mortars except for the exclusion of sand. For ultrasonic mixing, NS and water were premixed in ultrasonic machine for dispersion of fine particles. Before paste mixing, all the materials including sonicated mixtures were pre-conditioned at 30 °C for 24 h. The mixing procedures for cement pastes were similar to those of the mortars.

Table 1
Physical properties and chemical compositions of materials.

		Portland cement	Slag	Silica fume	Type 1 nano-silica	Type 2 nano-silica
Chemical composition (%)	CaO	63.4	41.8	0.2	–	–
	SiO_2	20.1	33.1	95.9	>99.8[a]	>99.8[a]
	Al_2O_3	4.1	13.7	0.3	–	–
	Fe_2O_3	3.3	0.7	0.3	–	–
	MgO	3.6	4.9	0.4	–	–
	Na_2O	0.22	0.2	0.05	–	–
	K_2O	0.43	0.5	0.6	–	–
	SO_3	2.1	0.7	0.2	–	–
	LOI	2.4	0.6	1.5	–	–
Mineral phases (%)	C_3S	66.8	–	–	–	–
	C_2S	7.3	–	–	–	–
	C_3A	5.3	–	–	–	–
	C_4AF	10.1	–	–	–	–
Physical properties (%)	Blain fineness (m^2/kg)	308	–	–	–	–
	BET surface area (m^2/g)	–	–	21.3	200.1	321.6
	Average primary particle size	28.2 μm	16.7 μm	150 nm[a]	12 nm[a]	7 nm[a]
	Specific gravity	3.15	2.94	2.2[a]	2.2[a]	2.2[a]

[a] Information provided by supplier.

Table 2
Mix proportions and flow values of slag mortars with different dosages of Type 1 nano-silica with specific surface area of 200.1 m^2/g (w/cm = 0.45).

Mix ID	% of nano-silica by mass of cementitious materials	Mixing procedure	Mix proportion					Super-plasticizer[a]	Flow (%)
			Water	Cement	Slag	Nano-silica	Sand		
Control	0	Mechanical	0.45	1.0	0	0	2.75	0.54	110
SL0	0	Mechanical	0.45	0.5	0.5	0	2.75	0.42	110
SL0.51	0.5	[b]	0.45	0.5	0.495	0.005	2.75	0.62	110
SL11	1.0	[b]	0.45	0.5	0.490	0.010	2.75	0.88	110
SL21	2.0	[b]	0.45	0.5	0.480	0.020	2.75	1.48	105

[a] % of (cement + slag + nano-silica) by mass.
[b] With ultrasonic premixing of nano-silica + water.

Table 3
Mix proportions of mortars for evaluating the effect of nano-silica size in comparison to that of silica fume (w/cm = 0.45).

Mix ID	Nano-inclusions	Mixing procedure	Mix proportion					Super-plasticizer[a]	Flow (%)
	Type		Water	Cement	Slag	Nano-inclusion	Sand		
SL1SF	Silica fume	Mechanical	0.45	0.5	0.49	0.01	2.75	0.42	107
SL11	Type 1 NS	[b]	0.45	0.5	0.49	0.01	2.75	0.88	110
SL12	Type 2 NS	[b]	0.45	0.5	0.49	0.01	2.75	1.04	111

[a] % of (cement + slag + nano-inclusion) by mass.
[b] With ultrasonic premixing of nano-silica + water.

Table 4
Mix proportions of mortars for evaluating mixing and dispersion methods of the nano-silica (w/cm = 0.45).

Mix ID	Mixing and dispersing procedure	Mix proportion					Super-plasticizer[a]	Flow (%)
		Water	Cement	Slag	Nano-silica	Sand		
SL11	[b]	0.45	0.5	0.49	0.01	2.75	0.88	110
SL11 (M)	Mechanical	0.45	0.5	0.49	0.01	2.75	1.17	104

[a] % of (cement + slag + nano-silica) by mass.
[b] With ultrasonic premixing of nano-silica + water.

Table 5
Mix proportions of concretes for evaluating the effect of nano-silica in comparison to that of silica fume (w/cm = 0.45).

Mix ID	Nano-inclusions	Mixing procedure	Mix proportion (kg/m^3)							Slump (mm)
	Type		Water	Cement	Slag	Nano-inclusion	Sand	Coarse aggregate	Super-plasticizer	
CSL0	–	Mechanical	180	200	200	0	774	1014	1.4	95
CSL2SF	Silica fume	[a]	180	200	192	8	771	1014	1.7	85
CSL21	Type 1 NS	[a]	180	200	192	8	771	1014	4.0	85

[a] With ultrasonic premixing of nano-inclusion + water.

2.3.2. Evaluate the rate of heat generation and cement hydration

Effect of NS on the rate of heat generation in cement pastes was evaluated according to ASTM C 1679 [13] by a Thermometric TAM Air 3115 isothermal calorimeter at a temperature of 30 °C. This temperature was selected to simulate weather conditions in tropical countries. The heat generation in the cement pastes reflects rate of cement hydration. The calorimeter was conditioned at 30 °C for a day before experiments, and amplifier range was set at 600 mW.

After the mixing, paste sample of about 10 g was transferred into a sample ampoule with the sample mass recorded. After capping the ampoule, the sample and reference ampoules were inserted into the calorimeter. The calorimeter started to record heat at about 15 min after the cementitious materials were in contact with water, thus the heat generated initially during mixing and preparation was not captured. The heat generated from the cement hydration was monitored continuously for 30 h. The power output (in mili-watt) from the calorimeter due to the heat generated was recorded every minute. The power output was normalized based on sample mass. The normalized power output was then converted to heat generated in the sample (in joules/gram).

2.3.3. Determining porosity and pore size distribution

The cement paste was cast in small plastic bottles and sealed with preheated wax and capped. The bottles were slowly rotated for the first 24 h to minimize segregation/bleeding and to ensure homogeneity of the cement paste sample. After that, the sample bottles were stored in the sealed condition at about 30 °C for curing.

At specified ages, the cement paste was removed from the bottles. Top and bottom part of the paste together with that in contact with inner wall of the bottle were removed by a chisel. The samples were broken into small pieces and dried in a vacuum oven at 50 °C until constant weight was reached.

Mercury intrusion porosimetry (MIP) was used to determine porosity and pore-size distribution of the mortars cured for 28 days. The test was performed using Micromeritics Autopore WIN9400 Series mercury porosimeter with a maximum pressure of 412.5 MPa. The minimum pore diameter reached under the maximum pressure was about 3.8 nm assuming a contact angle of 141.3° and a mercury surface tension of 0.485 N/m. Approximately 1.5 g of the hardened cement paste sample (3–5 mm in size) were used for each test.

2.3.4. Scanning electron microscopy

The microstructure of the concrete specimens CSL0 and CSL21 was examined to determine the influence of NS addition. 25 mm thick discs were cut from 100 mm × 200 mm concrete cylinders after 28 days of moist curing. They were dried in a vacuum oven at 50 °C until constant weight was reached. A 25 mm square specimen was cut from the concrete disc using a diamond precision cutter. The specimen was then impregnated with epoxy, polished and sputter coated. Scanning Electron Microscope (SEM) examination was carried out in the backscattered electron mode using an Apex Personal SEM. Energy dispersive X-ray was also used to identify the phases.

3. Results and discussion

3.1. Compressive strength development

3.1.1. Effect of nano-silica dosage on strength development of mortars

Compressive strength development of the slag mortars incorporating different dosages of Type 1 NS is given in Fig. 1 in comparison to that of control Portland cement mortar and reference mortar with 50% slag. The mortar with 50% slag had lower compressive strengths than the Portland cement mortar from 1 to 91 days as expected. However, the compressive strength of the slag mortars increased with the increase in NS dosages up to 91 days.

Percentage of strength increases of the mortars with the NS compared with the reference mortar with 50% slag is summarized in Table 6. With 2% NS, the compressive strength of the slag mortar increased by 39% and 30% at 3 and 7 days, respectively. The slag mortar with 2% NS had almost the same strength as the Portland cement mortar at 7 days, and exceeded strengths of the latter at 28 and 91 days. It is noted that the incorporation of the NS had less significant effect on the 1-day strength of the slag mortars than at 3 and 7 days. This might be related to the higher dosages of the superplasticizer used which had retarding effect in the mortars with NS to achieve a given workability.

3.1.2. Effect of particle size of nano-silica on strength development of mortars

Fig. 2 shows the effect of NS size on the compressive strength of the slag mortar compared to that with silica fume. With the incorporation of 1% NS and silica fume, the compressive strengths of the slag mortars were increased. The compressive strengths of the slag mortars were generally increased with the decrease in the particles size of SiO_2 inclusions from 1 to 91 days. With 1% NS with particle size of 7 nm, the compressive strengths of the slag mortars were increased by 35% and 21% at 3 and 7 days, respectively (Table 6). The increased early strengths with the incorporation of smaller size silica may be related to their high specific surface areas that increased rate of cement hydration and pozzolanic reaction. The results are consistent with findings by Qing et al. [1].

3.1.3. Effect of mixing and dispersion method on strength development of mortars

Effects of mixing and dispersion methods on the compressive strength development of slag mortars are shown in Fig. 3. No significant difference was observed in compressive strength development of mortars prepared by ultrasonicated NS with water and mechanical mixing method. However, careful examination of the data shows that the density of the mortar prepared by ultra-sonication of nano-silica (2231 kg/m^3) was lower than that prepared by mechanical mixing (2275 kg/m^3). The difference on the density of the mortars might have effect on the strength. This will be discussed further in the Section 3.3.3.

3.1.4. Strength development of slag concrete with nano-silica

Compressive strength development of the slag concrete with 2% Type 1 NS is shown in Fig. 4 in comparison to that of the reference slag concrete and concrete with the same amount of silica fume. Percentage of the strength increase of the slag concrete with 2% NS or silica fume compared with the reference slag concrete is summarized in Table 6. The results show that the early strengths of the concrete with the NS were increased by 22% and 18% at 3 and 7 days, respectively, whereas those with silica fume were increased by 4% and 5%, respectively, in comparison to those of the reference slag concrete. However, at the ages of 28 and 91 days, the three concretes had similar strength. This might be attributed to the coarse aggregate used which appears to have reached its strength limit at about 70 MPa in the slag concretes.

In ordinary concrete, interface transition zone (ITZ) between the coarse aggregate and mortar matrix is usually the weakest link. As a result, cracks generally go through the ITZ around coarse aggregate particles. With reduction of w/c and use of fine mineral admixture such as NS or silica fume, the ITZ and mortar matrix can be improved substantially. Thus, the strength of the concrete can be improved. However, if the strengths of the ITZ and mortar

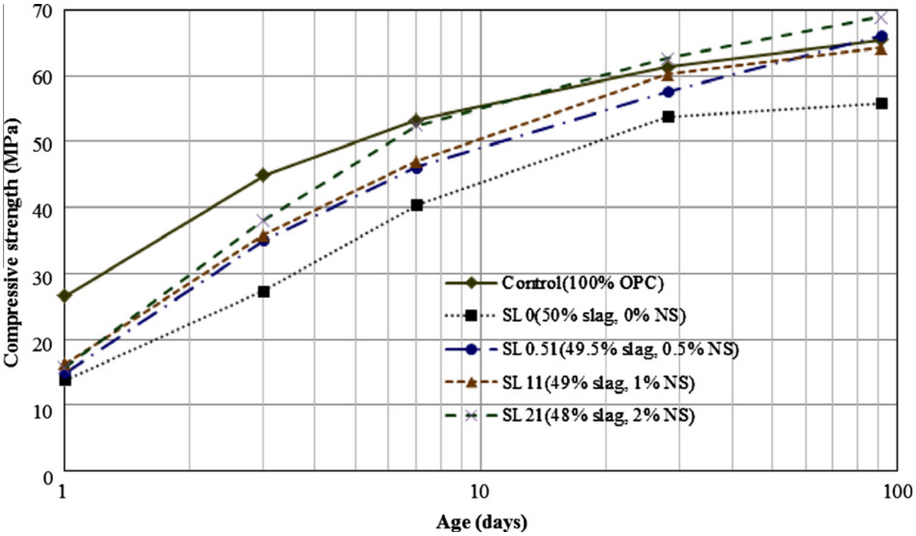

Fig. 1. Effect of the Type 1 nano-silica dosage on the compressive strength development of mortars.

Table 6
Strength increases of the mortars and concretes with nano-silica or silica fume compared with reference mortar and concrete with 50% slag.

Mix ID	Mortar, % of strength increases compared with reference mortar with 50% slag (SL0)				
	1d	**3d**	**7d**	**28d**	**91d**
SL0.51	8	28	14	7	18
SL11	18	31	16	12	15
SL21	14	39	30	17	23
SL1SF	10	17	14	11	13
SL11	18	31	16	12	15
SL12	29	35	21	17	20
SL11	18	31	16	12	15
SL11(M)	15	31	17	10	14
	Concrete, % of strength increases compared with reference concrete with 50% slag (CSL0)				
	1d	**3d**	**7d**	**28d**	**91d**
CSL2SF	–	4	5	1	1
CSL21	–	22	18	3	3

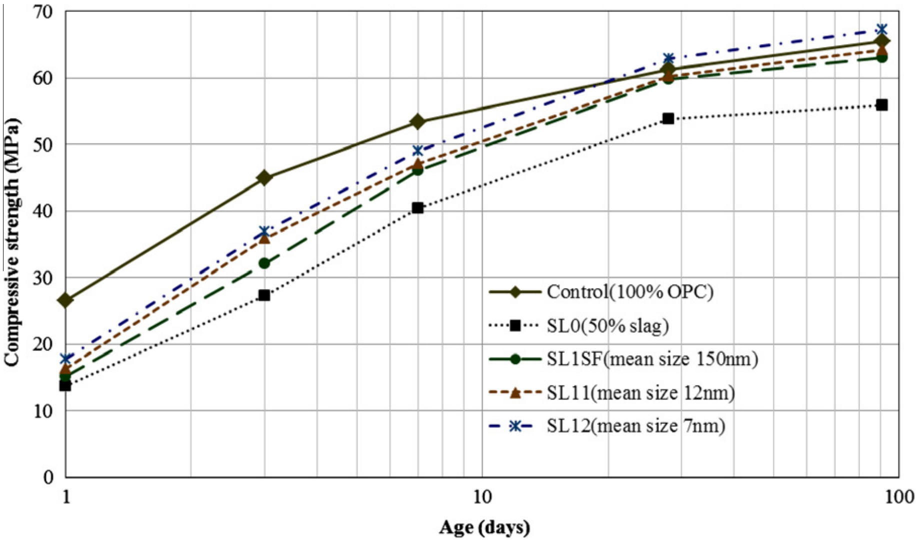

Fig. 2. Effect of the particle size of nano-inclusion on the compressive strength development of mortar (nano-silica and silica fume contents are 1% of cementitious materials by mass).

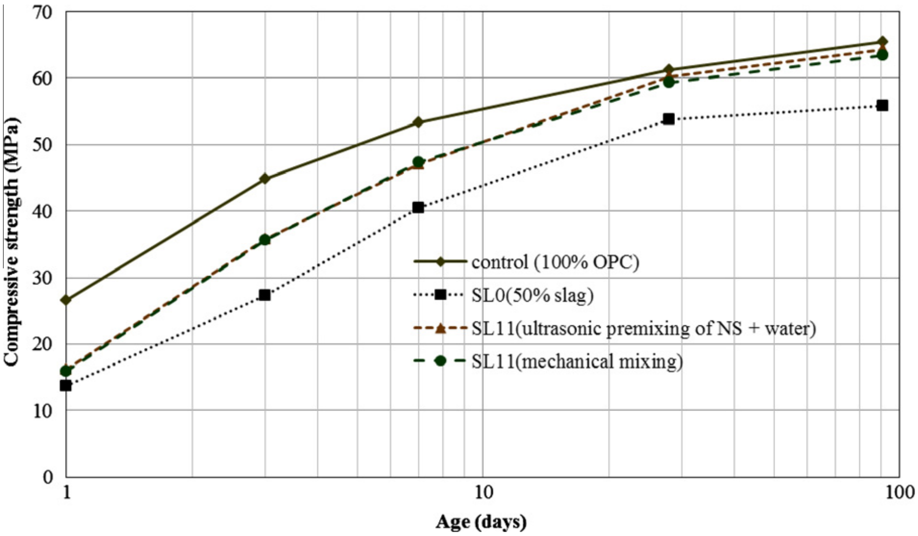

Fig. 3. Effect of mixing and dispersing method on the compressive strength development of mortar with 1% Type 1 nano-silica.

matrix are improved to such extents that coarse aggregate becomes the weakest link in concrete, crack will go through the coarse aggregate particles. In such conditions, reducing w/c and using fine mineral mixtures will no longer increase the concrete

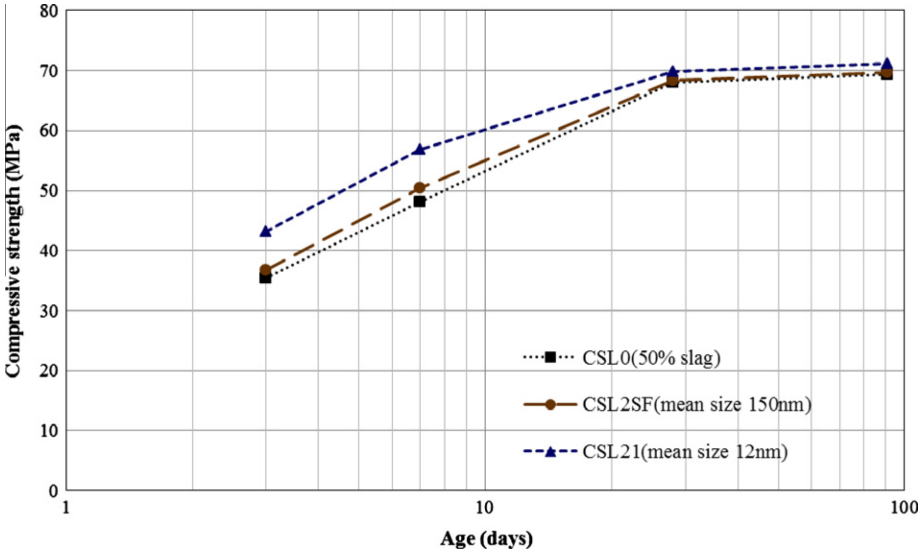

Fig. 4. Compressive strength development of concrete with 2% nano-silica in comparison to that of the reference concrete and concrete with the same amount of silica fume.

strength because coarse aggregate is a limiting factor for the strength of concrete. Fig. 5 shows that cracks went through coarse aggregate particles in the slag concrete with 2% NS after a compression test. This might explain why the strength of the slag concrete with 2% NS was not higher than that of the reference slag concrete and concrete with 2% silica fume.

3.1.5. Discussion on strength development due to the use of nano-silica or silica fume

Both the NS and silica fume are nano-sized highly reactive silica, and the average primary particle size of the former is about 10 times smaller than that of the latter. The mechanisms by which silica fume modifies cement paste, mortar, and concrete are summarized in ACI Committee 234 report [14]. These mechanisms are also applicable to NS. As the particle sizes of the NS are much smaller than those of the silica fume, the physical and chemical effect of the former is likely more substantial than the latter.

3.1.5.1. Physical effect. From physical perspective, extremely fine particle size of the NS may have accelerated cement and slag hydration by providing high amount of nucleation sites for precipitation of cement hydration products in the high-volume slag concrete. In the slag concrete, the accelerated cement hydration may also result in increased amount of calcium hydroxide in solution which may activate and speed up slag hydration.

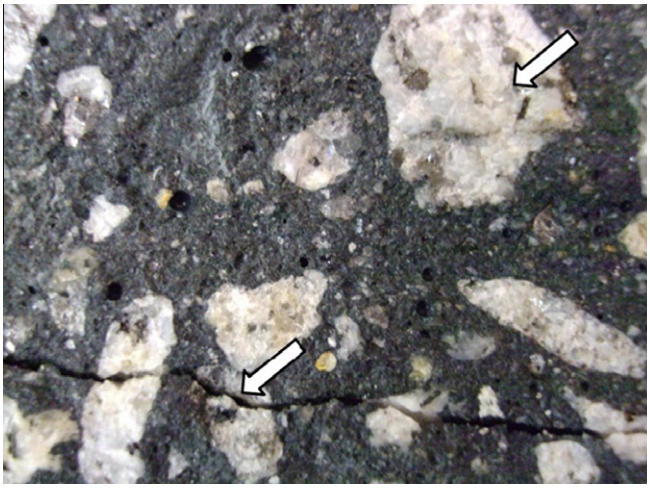

Fig. 5. Crack pattern in slag concrete with 2% nano-silica under compressive load. Crack goes through coarse aggregate particles.

In addition to the nucleation effect, NS may have acted as reactive filler which reduces bleeding and increases packing density of solid materials by occupying space between cement and slag particles. These physical effects of the NS may have contributed to the increased early strength of the slag concrete observed. However, as both the NS and silica fume are finer than Portland cement and slag the filler effect of the NS and silica fume may be similar.

3.1.5.2. Chemical effect. From chemical point of view, NS is highly reactive pozzolanic material and reacts with calcium hydroxide (CH) from cement hydration to form calcium silicate hydrate (C–S–H). Zhang and Gjørv [15] reported pozzolanic reaction of silica fume as early as 1-day of cement hydration. Since the NS had specific surface area about 10 times higher than that of silica fume, the pozzolanic reaction of the NS might have started before 24 h. The pozzolanic reaction of the NS at very early age might have also contributed to the increase early strength of the slag concrete observed. However, it was reported that addition of silica fume progressively reduced the alkalinity of Portland cement-silica fume system after 1 day of hydration [16] which is attributed to pozzolanic reaction of silica fume. As the NS is a highly reactive pozzolanic material, addition of the NS may reduce the alkalinity of the pore solution and consequently reduced the slag reaction.

3.1.5.3. Microstructure modification. In terms of microstructure modifications, the NS might reduce porosity in cement paste and in ITZ between the cement paste and aggregate due to the physical and chemical effects discussed above. It is also reported that NS can reduce CH crystal size in the ITZ more effectively than silica fume [17]. The above effects increase the density of the cement paste and improved bonding between the cement paste and aggregate (will be discussed in Sections 3.4 and 3.5) which might have contributed to the strength development.

3.2. Setting time of concrete

Fig. 6 shows the effect of NS on initial and final setting times of the slag concrete in comparison to the reference slag concrete and

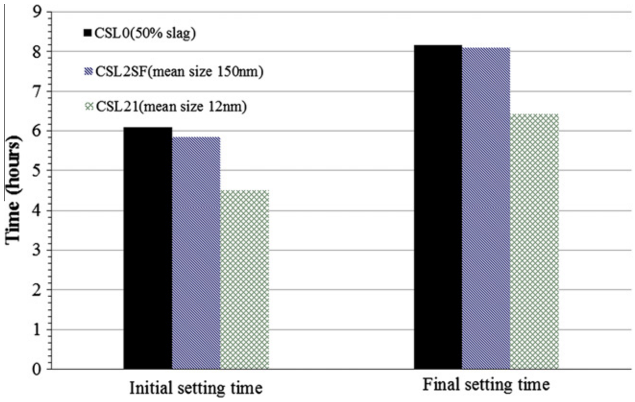

Fig. 6. Setting time of concrete with 2% nano-silica in comparison to that of the reference concrete and concrete with the same amount of silica fume.

concrete with silica fume. Results show reduction of initial and final setting times of 95 min and 105 min, respectively, when 2% NS was used in comparison to the reference slag concrete. However, incorporation of 2% silica fume did not affect the initial and final setting time significantly compared to those of the reference slag concrete. The reduction of the setting times of the NS concrete may be related to the finer particle size and higher surface area of the NS compared with those of silica fume which reduced the dormant period and increased cement hydration (will be discussed in the next section).

3.3. Rate of heat development

3.3.1. Effect of nano-silica dosage

Fig. 7 shows effects of NS dosage on the rate of heat development of cement pastes for the first 30 h, and the inset shows the corresponding cumulative heat development. A curve of cement paste without the slag and NS is included for comparison.

The calorimeter curves of the pastes with slag were very different from that of the control Portland cement paste without slag. Hydration of mixtures of Portland cement and slag is generally a two-stage reaction [18]. During early hydration, predominant reaction is with alkali hydroxide corresponding to Portland cement hydration (peak 2). Subsequent reaction is predominantly with calcium hydroxide which represents slag hydration (Peak 3). Fig. 5 clearly shows this two-stage reaction with slag hydration lag behind Portland cement hydration.

Results show that the length of dormant period was shortened with the incorporation of the NS in the slag cement pastes. Peaks 2 and 3 shifted to left with the incorporation of the NS in the pastes, suggesting accelerated Portland cement and slag hydration, respectively. The accelerated cement hydration might be due to increased nucleation sites provided by the fine NS particles. Whereas the accelerated slag reaction might be attributed to increased cement hydration and thus increased calcium hydroxide in solution at early age. There was no definite trend with respect to the dosage of NS due to the effect of retardation when higher dosage of superplasticizer was used in paste with increased NS dosage to achieve a given workability.

At 30 h cumulative heat generated in the cement paste increased with the increase in NS dosage which suggests increased cement hydration. This seems to be consistent with the slight increase in 1-day strength shown in Fig. 1. With the incorporation of 2% NS, the length of dormant period was reduced and cumulative heat development was increased with time compared with reference slag paste. These are consistent with the reduced setting times of concrete with NS observed in Fig. 6.

Maximum rate of heat development shown in Fig. 7 was reduced substantially with replacing 50% Portland cement by slag as expected. However, the length of the dormant period was reduced with the incorporation of slag. This was contrary to findings by other researchers [19,20], and might be due to the higher dosage of superplasticizer in the control cement paste with 100% Portland cement than in the reference slag paste with 50% slag (SL0).

3.3.2. Effect of particle size of nano-silica

Effect of NS particle size on the heat development of cement pastes is shown in Fig. 8. Peak 2 shifted to left and the length of the dormant period was shortened with the reduction of NS size and increase in specific surface area. The shortened dormant period was probably due to the nucleation effect of finer particle size of NS. For given amount of NS or silica fume added, the smaller the particle size, the more number of particles are available to act as nucleation sites for precipitation of hydration products. However, the changes of the peak 2, and dormant period were not significant for the different pastes. This was again due to the fact that dosage of superplasticizer was increased with the reduction of NS size in

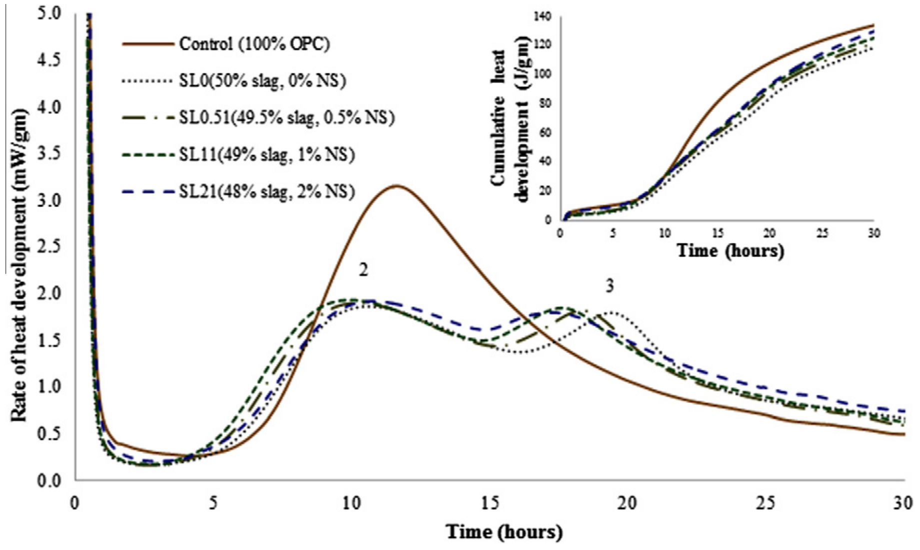

Fig. 7. Effect of the Type 1 nano-silica dosage on the rate of heat development in cement pastes.

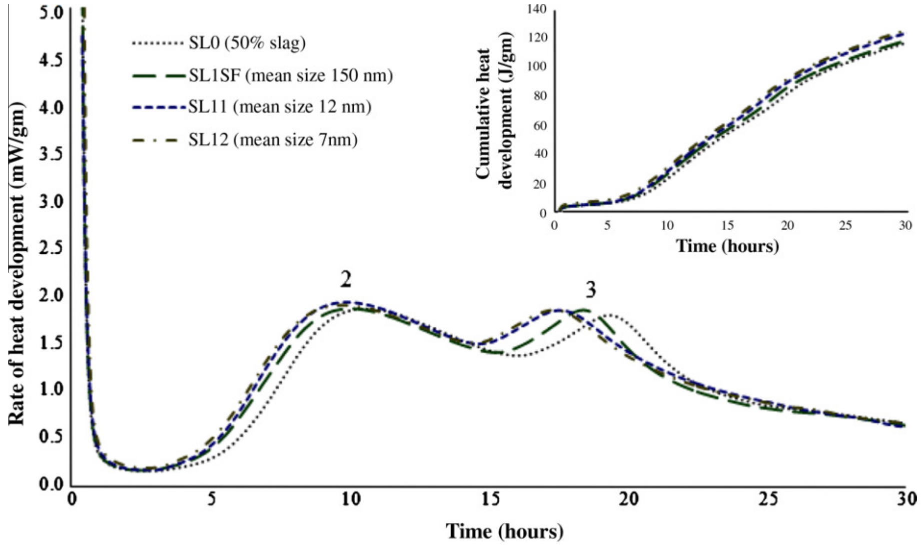

Fig. 8. Effect of the particle size of nano-inclusion on the rate of heat development in cement paste (nano-silica and silica fume contents are 1% of cementitious materials by mass).

order to achieve a given workability, and the superplasticizer used has retarding effect.

With decreasing particle size of NS, peak 3 of the heat development curve also shifted to the left. This may be explained by the increased amount of calcium hydroxide formed due to the acceleration of cement hydration by finer size of NS which substantially activated the hydration of slag at early age. However, the magnitude of the peak 3 was not significantly increased by finer NS.

Cumulative heat at 30 h increased with the reduction in particle size of NS and silica fume. This seems to be consistent with the observation of 1-day strength shown in Fig. 2. Moreover, the reduced dormant period and increased rate of heat development were consistent with the setting time of the concretes discussed in the previous section.

3.3.3. Effect of mixing and dispersion method

Effect of mixing and dispersing method of NS on the rate of heat development of cement paste is shown in Fig. 9, and the corresponding cumulative heat development is shown in the inset. For the paste with NS and water premixed with ultrasonic equipment, the dormant period was reduced and both peaks 2 and 3 occurred before those of the reference slag paste (SL0). For the paste prepared by mechanical mixing, however, the length of dormant period increased, and peaks 2 and 3 appeared later than those of the reference slag paste. The phenomena observed for the paste by mechanical mixing might be related partly to dispersion of NS and partly to the retarding effect due to higher dosage of superplasticizer used. The NS particles are very small and will agglomerate due to high surface interaction. The agglomeration of the NS might have resulted in decreased nucleation effect.

Cumulative heat generated within the first 24 h in the cement paste with ultrasonicated NS was higher than that with NS mechanically mixed with other ingredients which suggests that the cement hydration was increased by the sonication of NS and water. However, compressive strength of the mortars prepared by these two methods was not significantly different at the age of 1-day as mentioned earlier. The difference between the cement pastes and mortars may be attributed to two possible reasons.

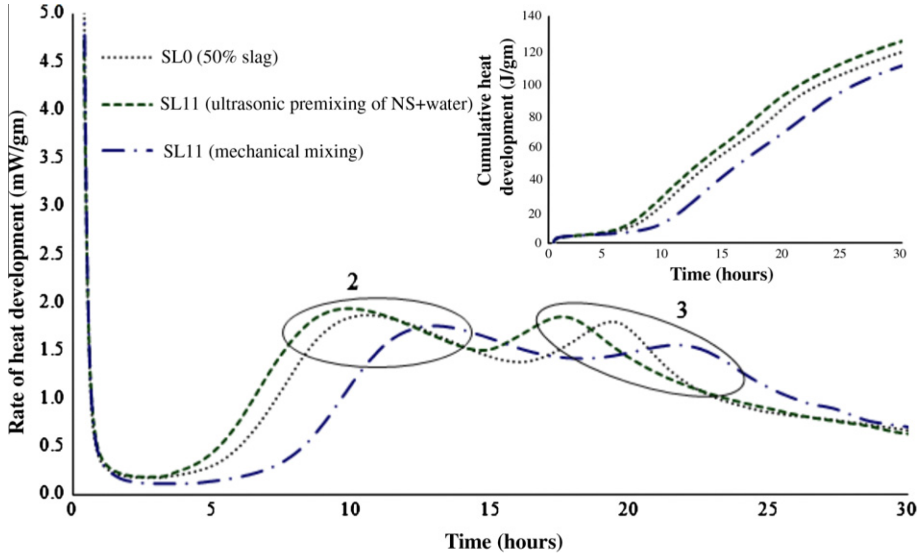

Fig. 9. Effect of mixing and dispersing method on the rate of heat development in cement paste with 1% Type 1 nano-silica.

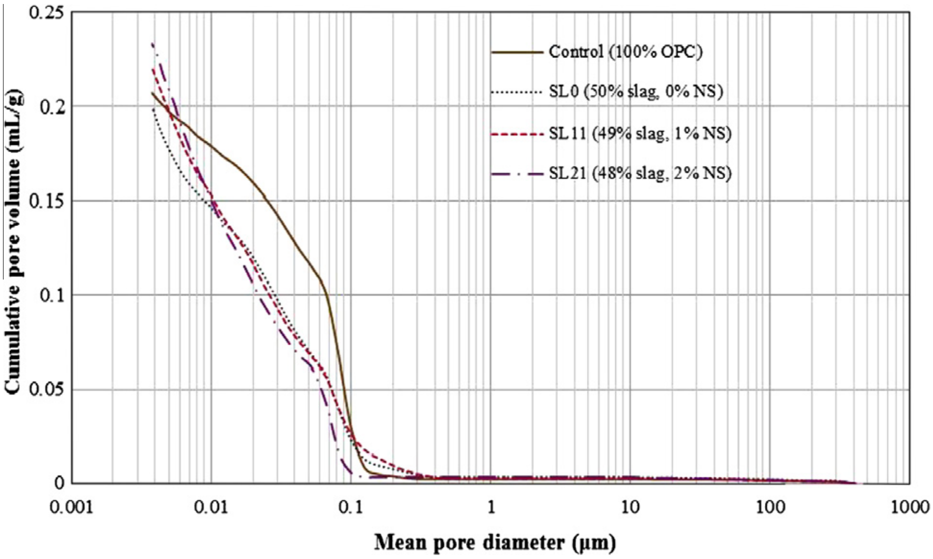

Fig. 10. Effect of the Type 1 nano-silica dosage on the porosity and pore size distribution in slag cement pastes.

Table 7
Porosity of high-volume slag cement pastes with nano-silica or silica fume compared with reference slag paste and control cement paste.

Mix ID	Large capillary porosity (%)	Medium capillary porosity (%)	Total capillary porosity (%)	Gel porosity (%)	Total porosity (%)	Threshold diameter (nm)	Critical pore diameter (nm)
Control	19.4	10.5	29.9	5.4	35.2	126	98
SL0	11.4	12.7	24.1	8.3	32.4	126	86
SL11	10.9	13.0	23.9	11.1	35.0	126	86
SL21	9.3	14.8	24.1	13.3	37.5	100	75
SL0	11.4	12.7	24.1	8.3	32.4	126	86
SL1SF	11.3	14.8	26.0	9.3	35.3	126	86
SL11	10.9	13.0	23.9	11.1	35.0	126	86
SL12	10.9	12.5	23.4	12.1	35.5	126	87
SL11	10.9	13.0	23.9	11.1	35.0	126	86
SL11(M)	11.2	13.3	24.5	10.5	35.0	126	86

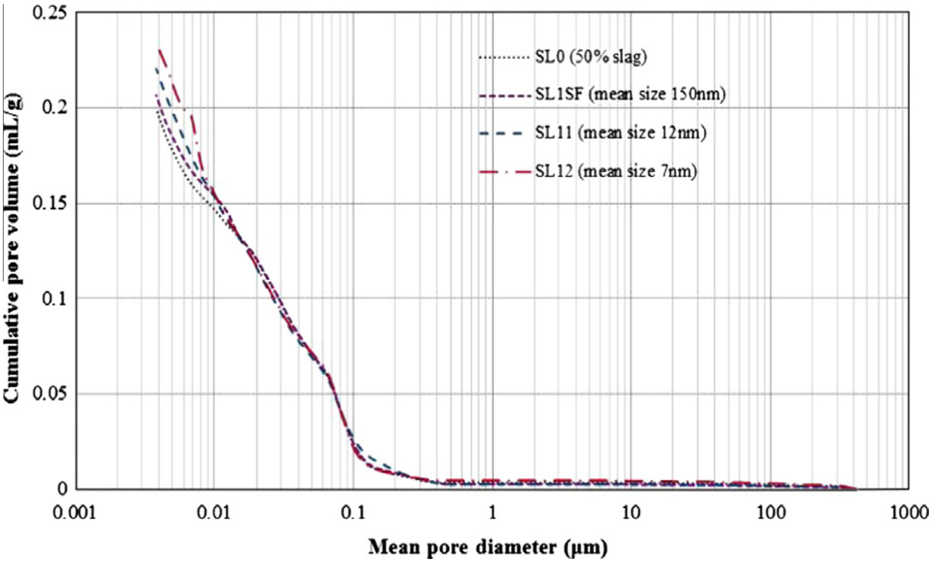

Fig. 11. Effect of the particle size of nano-inclusion on the porosity and pore size distribution in slag cement paste (nano-silica and silica fume contents are 1% of cementitious materials by mass).

First, the lower density of the mortar prepared by the ultrasonication of nano-silica (SL11) might have resulted in lower compressive strength. This suggests that if the density of the two mixtures SL11 and SL11(M) was the same, the former might have higher strength than the latter, consistent with the heat and rate of cement and slag hydration. The lower density of the mortar

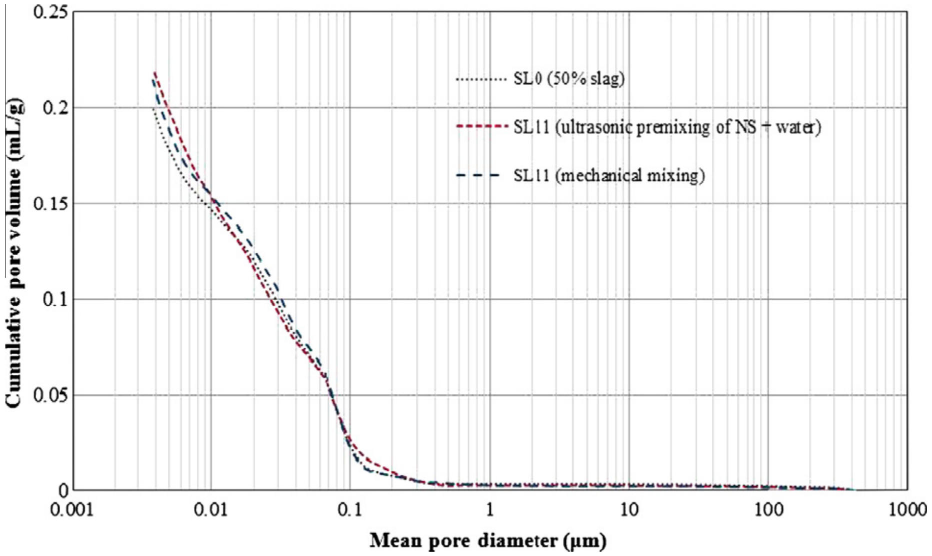

Fig. 12. Effect of mixing and dispersing method on the porosity and pore size distribution in slag cement paste with 1% Type 1 nano-silica.

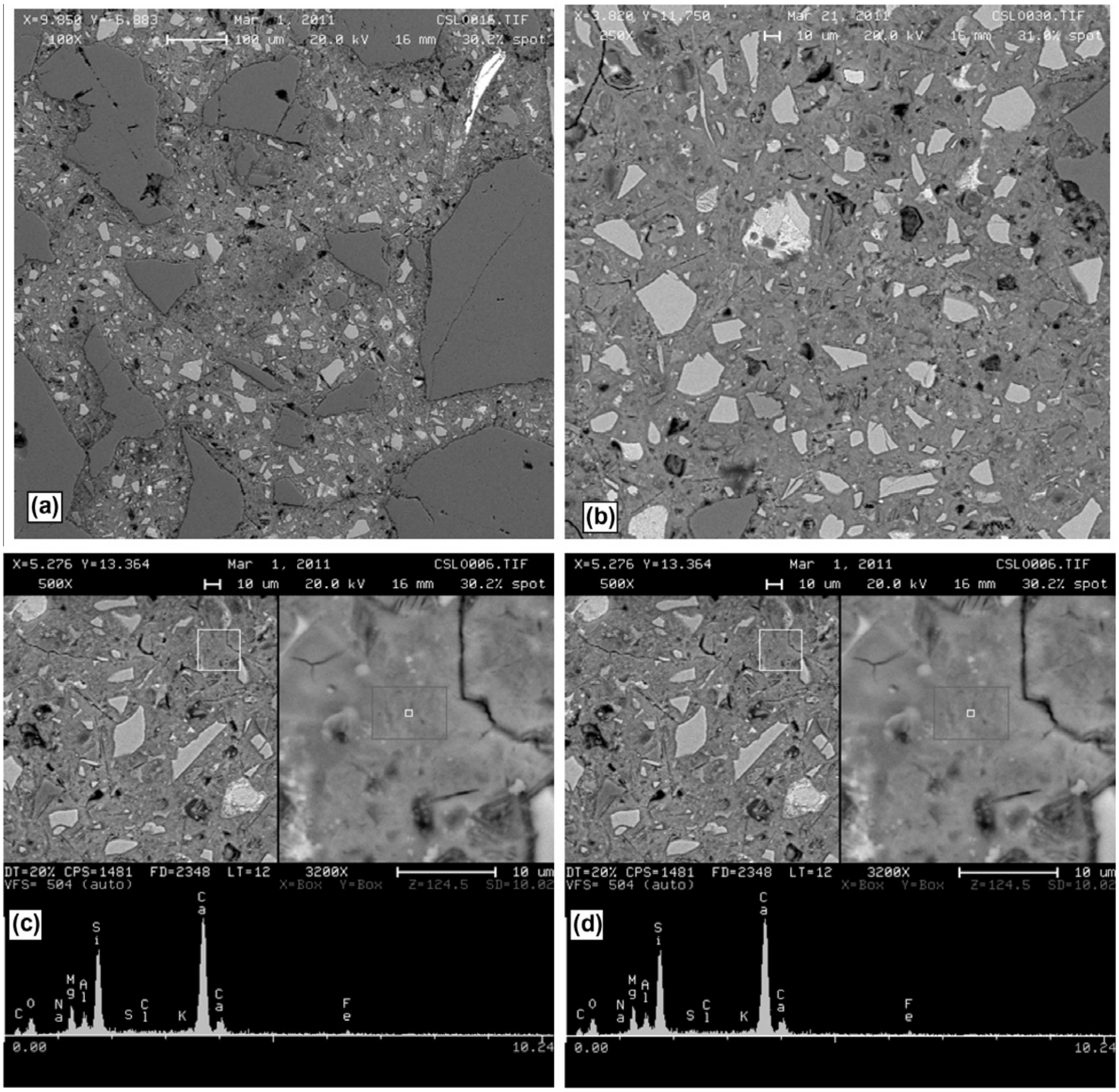

Fig. 13. Typical micro-structural characteristics of reference concrete with 50% slag (CSL0) (a) paste aggregate bonds (b) hardened paste showing the residual slag particles and (c and d) Ca/Si ratio of the C–S–H gel.

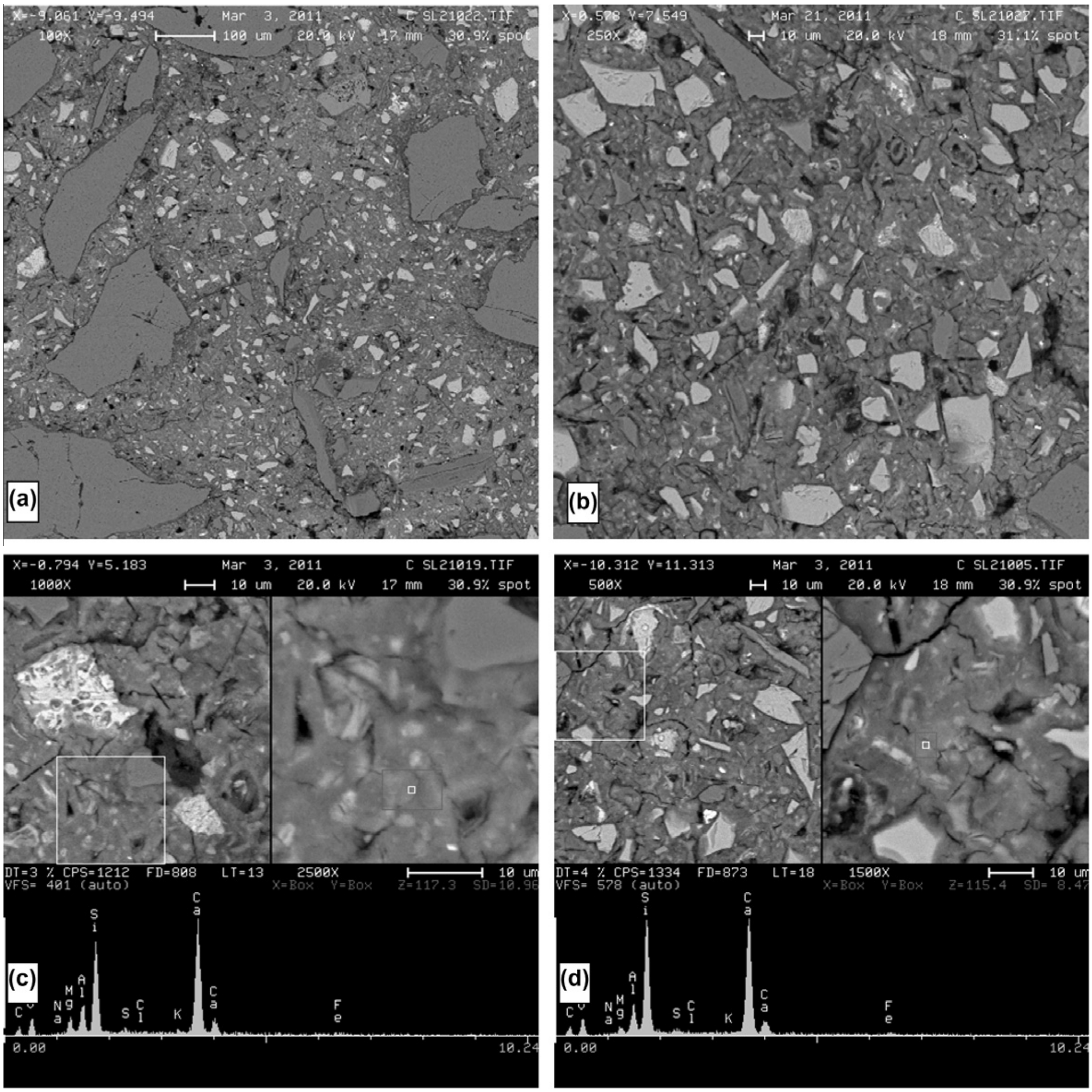

Fig. 14. Typical micro-structural characteristics of 2% nano-silica added slag concrete (CSL21) (a) paste aggregate bond (b) hardened paste showing the residual slag particles and (c and d) Ca/Si ratio of the C–S–H gel.

SL11 might be due to inadequate consolidation. Second, sand in mortar mixtures might have broken down the NS agglomerates, thus the NS particles might have been dispersed better in mortar than in cement paste. Thus the strength of SL11(M) might be less affected by the agglomeration of NS particles.

3.4. Porosity and pore-size distribution of pastes

3.4.1. Effect of nano-silica dosage

Effect of NS on pore size distribution of the various high-volume slag cement pastes at 28 days is shown in Fig. 10. The corresponding porosimetry data of various pastes are shown in Table 7. According to Mindess et al. [21], the pores in cement paste are divided into large capillary pores from (10–0.05 μm), medium capillary pores (0.05–0.01 μm) and gel pores (<0.01 μm). The gel pores are the intrinsic porosity of C–S–H. The mercury intrusion porosimeter used in this study was able to detect pores with diameter down to 0.0038 μm.

The results show that large capillary porosity of slag paste was decreased, whereas medium capillary porosity was increased with increasing dosage of the NS. The total capillary porosity of the slag pastes, however, was not affected significantly by the incorporation of the NS. Threshold and critical pore diameters were not affected by the incorporation of 1% NS, but were decreased with the inclusion of 2% NS. The threshold pore diameter is a diameter at first inflection point of volume–diameter curve which indicates the minimum diameter of pores that are continuous through the paste [21,22]. The critical pore diameter is a diameter at which the slope of the volume–diameter curve is the steepest and corresponds to the mean size of pore entryways that allows maximum percolation throughout the pore system [21]. Since permeability and penetration of harmful substances into the concrete are affected mainly by the large and medium capillary pores, the incorporation of 1% NS in the slag concrete may not affect such concrete properties significantly. Thus, 2% NS was used for concrete mixtures.

The gel pores of the slag pastes were increased with the increase in the NS dosage, thus the total porosity of the slag pastes was also increased.

Compared with control Portland cement paste, the pastes with high volumes of slag had lower large and total capillary porosities and critical pore diameter, but higher gel porosity. These will contribute to high resistance of slag concretes against penetration of

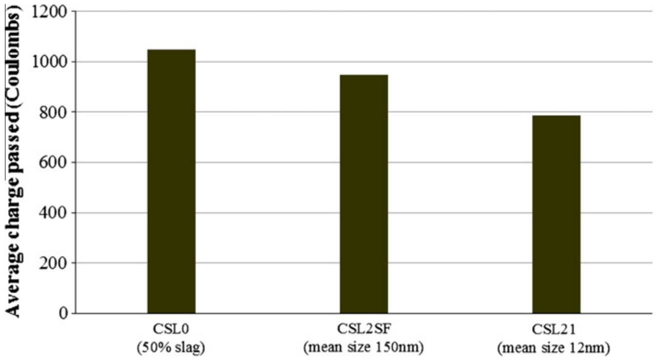

Fig. 15. Effect of the particle size of nano-inclusions on charge passed in concrete at 28 days (nano-silica and silica fume contents are 2% of cementitious materials by mass).

harmful substances and good durability which has been reported in numerous cases [18].

Mechanism of reduced large capillary porosity in the slag pastes incorporating NS may be explained by physical and chemical effects attributed by NS (as described in Section 3.1.5) similar to those with the use of silica fume in cement pastes as described in ACI Committee 234 Report [14]. Nano-silica made the pore structure of paste more homogeneous by decreasing large but increasing medium capillary porosities. The increased gel porosity might have resulted from the increased amount of C–S–H in the paste.

Nevertheless, limitations of MIP method should be noted in evaluation of pores structure of cement based materials. Besides the required pore shape assumption, "ink-bottle" or "neck-bottle" [23] effect has been found to have significant influences on the pore size distributions. Diamond [24] further limited MIP credit only to threshold diameters and intruded pore space measurements.

3.4.2. Effect of particle size of nano-silica

Fig. 11 shows effect of particle size of NS on porosity and pore-size distribution of high-volume slag cement pastes at 28 days in comparison to that of the reference slag paste and paste with the same amount of silica fume. The porosimetry data of the slag pastes are summarized in Table 7. The results indicated that the incorporation of the NS with mean sizes of 7 and 12 nm and silica fume did not have significant effect on large, medium, and total capillary porosities and threshold and critical diameters of the slag pastes. However, the gel porosity was increased slightly with the decrease of mean particle sizes of the silica inclusions.

3.4.3. Effect of mixing and dispersion method

Effects of mixing and dispersion methods of the NS on porosity and pore-size distribution of the slag cement pastes are shown in Fig. 12 with summary of capillary and gel porosity and threshold and critical pore diameters given in Table 7. The results indicate that using ultrasonic premixing of NS and water or mechanical mixing of all ingredients did not have significant effect on pore structure of the slag pastes.

3.5. Microstructure of slag concrete at 28 days

Fig. 13a–d show typical scanning electron micrographs obtained from a 28 days old reference high volume slag concrete (CSL0). From these Micrographs, it can be seen that most of the fine cement grains were completely hydrated by 28 days of curing. However, many residual slag grains were identified in the concrete (Fig. 13a and b), which indicates that the slag grains were either not hydrated or only partially hydrated. The hardened paste matrix was dense with some residual slag grains. The Ca/Si ratio of the C–S–H gel was found to be approximately 1.3–1.7. The aggregate paste interface was found to be porous (Fig. 13a).

Fig. 14a–d shows microstructure of the slag concrete with 2% NS in the mixture (CSL21). The degree of slag hydration appeared to be lower compared to the reference sample without NS, whereas the degree of cement hydration appeared to be higher as a result of NS addition. The reduced slag hydration may be attributed to the high pozzolanic activity of the NS which progressively reduced the alkalinity of pore solution and consequently reduced the slag reaction as mentioned in Section 3.1.5.2. The Ca/Si ratio of the C–S–H gel was determined to be 1.0–1.2, which was lower than that found in the reference high-volume slag concrete (CSL0). This could be due to the presence of more amorphous silica in the system that in turn increased the Si content of the C–S–H gel. The aggregate and paste interface was denser and continuous compared with the reference slag concrete (CSL0) mainly due to the effects of the NS on the interface described in Section 3.1.5.

3.6. Resistance to chloride-ion penetration

Resistance of concrete to chloride-ion penetrability is shown in Fig. 15. The concrete with 2% NS had lower charge passed in comparison to that with the same amount of silica fume. However, both of the concrete had charge passed below 1000 coulombs, which is considered "very low" according to ASTM C 1202. Both of them had lower charge passed in comparison to the concrete without NS or silica fume. According to Halamickova et al. [25] the coefficient of chloride-ion diffusion varied linearly with the critical pore diameter. The reduced charge passed through the slag concrete incorporating 2% NS was consistent with the reduced critical and threshold pore diameters, and improved microstructure discussed in previous sections.

4. Conclusions

Based on the experimental results using nano-silica in high-volume slag pastes, mortars and concretes with w/cm of 0.45, following conclusions can be drawn:

1. Length of dormant period was shortened, and rate of cement and slag hydration were accelerated with the incorporation of the NS in the high-volume slag cement pastes.
2. Compressive strength of the slag mortars were increased with the increase in NS dosages from 0.5% to 2.0% by mass of cementitious material at various ages up to 91 days.
3. The strengths of the slag mortars were generally increased with the decrease in the particles size of silica inclusions at early age.
4. Ultra-sonication of nano-silica with water is probably a better method for proper dispersion of nano-silica than mechanical mixing method.
5. The incorporation of 2% NS by mass of cementitious materials reduced initial and final setting time by 95 and 105 min, and increased 3- and 7-day compressive strengths of high-volume slag concrete by 22% and 18%, respectively, in comparison to the reference concrete with 50% slag.
6. With the increasing dosage of NS, large capillary porosity was decreased, whereas medium capillary porosity was increased in the slag cement pastes at 28 days. However, the total capillary porosity of the slag pastes was not affected significantly by the incorporation of the NS. Threshold and critical pore diameters in slag cement pastes were not affected by the incorporation of 1% NS, but were decreased with the inclusion

of 2% NS. No significant difference in pore structure was observed among the slag pastes with different particle sizes of silica, and among those prepared by ultrasonicated NS with water and by mechanical mixing method.

7. The incorporation of 2% NS by mass of cementitious materials densified the paste-aggregate interface compared with the reference slag concrete without NS addition.
8. The 28-day charge passed through the slag concrete with NS was lower than that of reference slag concrete.
9. Nano-silicas with mean particle sizes of 7 and 12 nm appear to be more effective in increasing the rate of cement hydration and reaction compared with silica fume. The NS reduced the setting times and increased early strengths of the high-volume slag concrete. However, the setting times and early strength of the high-volume slag concrete were not affected by the silica fume significantly. The charge passed through the high-volume slag concrete with NS was similar to that of concrete with silica fume.

Acknowledgments

Grateful acknowledgment is made to National University of Singapore for providing partial scholarship to the second author. Appreciation is made to past undergraduate student Mr. Huynh Thanh Binh, Structure Laboratory Technologist Mr. Ang Beng Oon and Research Fellow Ms. Li Wei who contributed to some of the experimental work.

References

[1] Qing Y, Zenan Z, Deyu K, Rongshen C. Influence of nano-SiO_2 addition on properties of hardened cement paste as compared with silica fume. Constr Build Mater 2007;21(3):539–45.

[2] Li H, Xiao H-G, Yuan J, Ou J. Microstructure of cement mortar with nano-particles. Compos B Eng 2004;35(2):185–9.

[3] Jo B-W, Kim C-H, Tae G-h, Park J-B. Characteristics of cement mortar with nano-SiO_2 particles. Constr Build Mater 2007;21(6):1351–5.

[4] Schoepfer J, Maji A. An investigation into the effect of silicon dioxide particle size on the strength of concrete. ACI Special Publication vol. 267(5), 2009. p. 45–58.

[5] Li G. Properties of high-volume fly ash concrete incorporating nano-SiO_2. Cem Concr Res 2004;34(6):1043–9.

[6] Said AM, Zeidan MS. Enhancing the reactivity of normal and fly ash concrete using colloidal nano-silica. ACI Special Publication vol. 267(7), 2009. p. 75–86.

[7] ASTM C 1202, Standard test method for electrical indication of concrete's ability to resist chloride ion penetration, Annual Book of ASTM Standards, vol. 04.02; 2008.

[8] ASTM C 33, Standard specification for concrete aggregates, Annual Book of ASTM Standards, vol. 04.02; 2008.

[9] ASTM C 1437, Standard test method for flow of hydraulic cement mortar, Annual Book of ASTM Standards, vol. 04.01; 2005.

[10] ASTM C 109/C 109M, Standard test method for compressive strength of hydraulic cement mortars (using 2-in or [50-mm] cube specimens), Annual Book of ASTM Standards, vol. 04.01; 2005.

[11] BS EN 12390-3, Testing hardened concrete – Part 3: compressive strength of test specimens, British Standards Institution; 2002.

[12] ASTM C 403/C 403M, Standard test method for time of setting of concrete mixtures by penetration resistance, Annual Book of ASTM Standards, vol. 04.02; 2008.

[13] ASTM C 1679, Practice for measuring hydration kinetics of hydraulic cementitious mixtures using isothermal calorimetry, Annual Book of ASTM Standards, vol. 04.02; 2008.

[14] ACI 234R, Guide for the use of silica fume in concrete, ACI Committee 234 Report; 2006.

[15] Zhang M-H, Gjørv OE. Effect of silica fume on cement hydration in low porosity cement pastes. Cem Concr Res 1991;21(5):800–8.

[16] Diamond S. Effects of microsilica (silica fume) on pore-solution chemistry of cement pastes. J Am Ceram Soc 1983;66(5):C-82–4.

[17] Qing Y, Zenan Z, Li S, Rongshen C. A comparative study on the pozzolanic activity between nano-SiO_2 and silica fume. J Wuhan Univ Technol – Mater Sci Edition 2006;21(3):153–7.

[18] ACI 233R, Slag cement in concrete and mortar, ACI Committee 233 Report; 2003.

[19] Roy DM, Idorn GM. Hydration, structure, and properties of blast furnace slag cements, mortars, and concrete. ACI Special Publication vol. 79(6), 1982. p. 444–57.

[20] Hwang C-L, Shen D-H. The effects of blast-furnace slag and fly ash on the hydration of Portland cement. Cem Concr Res 1991;21(4):410–25.

[21] Mindess S, Young JF, Darwin D. Concrete. 2nd ed. Upper Saddle River, NJ: Prentice Hall; 2003.

[22] Winslow DN, Diamond S. A mercury porosimetry study of the evolution of porosity in Portland cement. J Mater 1970;5(3):564–85.

[23] Diamond S, Leeman ME. Pore size distributions in hardened cement paste by SEM image analysis. Mater Res Soc Symp Proc 1995;370:217–26.

[24] Diamond S. Mercury porosimetry: an inappropriate method for the measurement of pore size distributions in cement-based materials. Cem Concr Res 2000;30(10):1517–25.

[25] Halamickova P, Detwiler RJ, Bentz DP, Garboczi EJ. Water permeability and chloride ion diffusion in Portland cement mortars: relationship to sand content and critical pore diameter. Cem Concr Res 1995;25(4):790–802.